Applied Mathematics & Information Sciences
An International Journal

http://dx.doi.org/10.18576/amis/100116

Reconstructions that Combine Cell Average Interpolation with Least Squares Fitting

Francesc Aràndiga and José Jaime Noguera*

Departament de Matemàtica Aplicada. Universitat de València, Spain

Received: 19 Jun. 2015, Revised: 17 Aug. 2015, Accepted: 18 Aug. 2015
Published online: 1 Jan. 2016

Abstract: In this paper we present two reconstructions in the cell average framework of multiresolution *a la Harten*. The first one combines interpolation and least squares fitting and the second one is based on least squares fitting. We study some of their properties as well as its approximation order. We also analyze how different adaptive techniques (*ENO* and *SR*) can be used within these reconstructions. We apply them to noise removal and compare the results that we obtain with other existing techniques.

Keywords: Cell average, Least squares, Interpolation, Nonlinear multiresolution, Denoising

1 Introduction

A common problem in approximation theory is the reconstruction of a function from a discrete set of data which gives information on the function itself. This information usually comes either as point-values or cell-averages of the function over a finite set of points or cells, respectively. The function is then approximated by an interpolant, that is, another function whose values or cell-averages at the given set of points or, respectively, cells, coincide with those of the original one.

The interpolation is a linear procedure of the values on the given set of points, but in this case the accuracy of the approximation in the presence of a singularity is limited by its order, so that any stencil crossing the singularity will result in an unsatisfactory approximation. This means that increasing the degree of the polynomial will produce larger regions of poor accuracy around singularities.

The choice of stencils that avoid crossing singularities, whenever this is possible, is crucial for the improvement of the accuracy of the approximation. This is the key underlying the *ENO* (essentially non-oscillatory) technique, introduced by Harten et al. [9] in the context of high resolution shock capturing (HRSC) schemes for conservation laws. With the *ENO* interpolant the region affected by each singularity is reduced to the interval that contains it, assuming the singularities are sufficiently well separated.

It is possible to improve this result using the Harten's subcell resolution technique (*SR*) ([1,2,7]). If the location of the singularity within the cell (or a sufficient good approximation of it) is known, then the loss of accuracy can be avoided.

In [3] we study the application of these reconstructions to the case where the data are contaminated with noise. On one hand we use interpolatory reconstructions and on the other hand we rely on least squares. We do not get good interpolants in all cases. This motivates us to introduce new reconstructions using both ideas.

The first one combines interpolation with approximation in the least squares sense (called in this paper *Interp-*$\mathscr{LS}$) and the second reconstruction is based, following [11], on approximate the data in the least square sense (called in this paper $\mathscr{LS}$). Here we present these reconstructions in the cell average framework which is more appropriate in the presence of noise. In [12] we can see these reconstructions in the point value context. We also analyze how can be used combined with different non linear techniques (*ENO* and *SR* see [7] and [9] resp.).

The paper is organized as follows: We recall in Section 2 the discrete framework for multiresolution introduced by Harten focusing on cell average discretizations. We introduce the *Interp-LS* reconstruction for cell averages in Section 3. There, we also present how this reconstruction can be combined with non-linear techniques. In Section 4 we present the least squares

* Corresponding author e-mail: arandiga@uv.es

© 2016 NSP
Natural Sciences Publishing Cor.

reconstruction for cell averages ($\overline{\mathscr{LSC}}$). Section 5 is devoted to show some numerical experiments where we can see the results that we obtain with the techniques presented in this paper. Finally, in Section 6 we present the conclusions.

2 Harten's framework for multiresolution analysis

The building blocks of a multiresolution analysis as described by Harten (see [8] and references therein) are a sequence of linear decimation operators $\{D_{k+1}^k\}_{k=0}^{L-1}$, a nested sequence of linear vector spaces V^{k+1}, with $D_{k+1}^k : V^{k+1} \longrightarrow V^k$ (which, from a vector of V^{k+1}, computes a coarser representation of it), and a sequence of prediction operators $\{P_k^{k+1}\}_{k=0}^{L-1}, P_k^{k+1} : V^k \longrightarrow V^{k+1}$ which, from a vector of V^k obtains an approximation to its (finer) representation in V^{k+1}. In most applications, V^{k+1} is a space of sequences of real numbers. Our description implies that the resolution increases with k. The decimation and prediction operators have to satisfy the compatibility condition:

$$D_{k+1}^k P_k^{k+1} = I_{V^k}. \tag{1}$$

Given $v^{k+1} \in V^{k+1}$, the *prediction error* $e^{k+1} = Q_{k+1}v^{k+1} := (I_{V^{k+1}} - P_k^{k+1}D_{k+1}^k)v^{k+1}$ obtains the information in $v^{k+1} \in V^{k+1}$ that cannot be predicted from $v^k = D_{k+1}^k v^{k+1} \in V^k$ by the operator P_k^{k+1}.

It is easily seen that the *error* vector, $e^{k+1} := Q_{k+1}v^{k+1}$, belongs to the null space of D_{k+1}^k, denoted by $\mathscr{N}(D_{k+1}^k)$ ([2]). Let $G_{k+1} : V^{k+1} \longrightarrow \mathscr{N}(D_{k+1}^k)$ be the operator which assigns to each vector $e^{k+1} \in V^{k+1}$ the coefficients d^{k+1} of its representation in terms of a given basis, $\{\mu_j^{k+1}\}$, of $\mathscr{N}(D_{k+1}^k) \subset V^{k+1}$, and let E_{k+1} be the canonical injection $\mathscr{N}(D_{k+1}^k) \hookrightarrow V^{k+1}$. Clearly $G_{k+1}E_{k+1} = I_{\mathscr{N}(D_{k+1}^k)}$ and $E_{k+1}G_{k+1} = I_{V^{k+1}}$. The *non-redundant* information in the error vector is contained in the set of coefficients $\{d_i^{k+1}\}$, called the scale coefficients at level k. We note that v^{k+1} and $\{v^k, d^{k+1}\}$ have the same cardinality.

These ingredients allow to construct an alternative representation of a vector $v^{k+1} \in V^{k+1}$. Given v^{k+1} we evaluate:

$$\begin{cases} v^k &= D_{k+1}^k v^{k+1}, \\ d^{k+1} &= G_{k+1}(I_{V^{k+1}} - P_k^{k+1}D_{k+1}^k)v^{k+1}, \end{cases} \tag{2}$$

and given v^k and d^{k+1}, computed by (2), the vector v^{k+1} is recovered by the inverse formula $v^{k+1} = P_k^{k+1}v^k + E_{k+1}d^{k+1}$.

This gives the equivalence between v^{k+1} and $\{v^k, d^{k+1}\}$. By repeating step (2) for v^k one obtains its corresponding decomposition $\{v^{k-1}, d^k\}$. Iterating this process from $k = L-1$ to 0 we find that a multiresolution setting $\{\{V^k\}_{k=0}^L, \{D_{k+1}^k\}_{k=0}^{L-1}\}$ and a sequence of corresponding prediction operators $\{P_k^{k+1}\}_{k=0}^{L-1}$ satisfying (1) define an invertible multiresolution transform.

In Harten's framework, the decimation and prediction operators are built from a sequence of discretization operators and a sequence of *compatible* reconstruction operators. Given a function belonging to a certain functional space $\mathscr{F}$ the discretization operator $\mathscr{D}_{k+1} : \mathscr{F} \longrightarrow V^{k+1}$ obtains a discrete representation of it at the resolution level defined by V^{k+1}. Conversely, the reconstruction operator $\mathscr{R}_{k+1} : V^{k+1} \longrightarrow \mathscr{F}$ obtains a function in $\mathscr{F}$ from discrete values in V^{k+1}. The reconstruction operators $\mathscr{R}_{k+1}$ are *compatible* with $\mathscr{D}_{k+1}$ provided that

$$\mathscr{D}_{k+1}\mathscr{R}_{k+1} = I_{V^{k+1}} \tag{3}$$

is satisfied for each k.

The decimation and prediction operators corresponding to these sequences are obtained as $D_{k+1}^k = \mathscr{D}_k\mathscr{R}_{k+1}$ and $P_k^{k+1} = \mathscr{D}_{k+1}\mathscr{R}_k$. The compatibility condition (1) is a consequence of (3).

In Harten's framework, the discretization process specifies the setting, then the choice of a reconstruction operator defines a multiresolution transformation whose properties are closely related to those of the reconstruction. From the point of view of data-compression applications, accuracy of the reconstruction is an important feature.

2.1 Cell average multiresolution analysis

Let $f \in \mathscr{F} = L^1([0,1])$. Considering the set of nested dyadic grids defined by

$$X^k = \{x_i^k\}_{i=0}^{N_k},\ N_k = 2^k N_0,\ x_i^k = ih_k,\ h_k = \frac{1}{N_k},\ k = 0,\ldots,L$$

where $N_0 \in \mathbf{N}$. The cell-average discretization operator $\mathscr{D}_{k+1} : \mathscr{F} \longrightarrow V^{k+1}$ is defined in [8] as follows:

$$\overline{f}_i^{k+1} := (\mathscr{D}_{k+1}f)_i = \frac{1}{h_{k+1}}\int_{x_{i-1}^{k+1}}^{x_i^{k+1}} f(x)dx, \quad 1 \le i \le N_{k+1}. \tag{4}$$

The decimation can then be computed by:

$$\overline{f}_i^k = \tfrac{1}{h_k}\int_{x_{i-1}^k}^{x_i^k} f(x)dx = \tfrac{1}{2h_{k+1}}\int_{x_{2i-2}^{k+1}}^{x_{2i}^{k+1}} f(x)dx = \tfrac{1}{2}(\overline{f}_{2i}^{k+1} + \overline{f}_{2i-1}^{k+1}). \tag{5}$$

Let $p_i(x)$ the polynomial of degree $r-1 = nr+nl$, $nr, nl \in \mathbf{N}$, such that

$$\frac{1}{h_k}\int_{x_{i+s-1}^k}^{x_{i+s}^k} p_i(x)dx = \overline{f}_{i+s}^k, \quad s = -nl,\ldots,nr, \tag{6}$$

then, the reconstruction is defined as follows:

$$\overline{\mathscr{IC}}_{nl,nr}^{r-1}(x; \overline{f}^k) = p_i(x),\ x \in [x_{i-1}^k, x_i^k],\ i = 1,\ldots,N_k.$$

© 2016 NSP
Natural Sciences Publishing Cor.

The prediction operator is in this case:

$$\left(P_k^{k+1}\overline{f}^k\right)_{2i-1} = \left(\mathscr{D}_{k+1}(\overline{\mathscr{IC}}^{r-1}_{nl,nr}(x;\overline{f}^k))\right)_{2i-1} = \frac{1}{h_{k+1}}\int_{x_{2i-2}^{k+1}}^{x_{2i-1}^{k+1}} \overline{\mathscr{IC}}^{r-1}_{nl,nr}(x;\overline{f}^k)dx,$$

$$\left(P_k^{k+1}\overline{f}^k\right)_{2i} = \left(\mathscr{D}_{k+1}(\overline{\mathscr{IC}}^{r-1}_{nl,nr}(x;\overline{f}^k))\right)_{2i} = \frac{1}{h_{k+1}}\int_{x_{2i-1}^{k+1}}^{x_{2i}^{k+1}} \overline{\mathscr{IC}}^{r-1}_{nl,nr}(x;\overline{f}^k)dx.$$

As a consequence of (6) we have

$$\frac{1}{2}\left(\left(P_k^{k+1}\overline{f}^k\right)_{2i-1} + \left(P_k^{k+1}\overline{f}^k\right)_{2i}\right) = \overline{f}_i^k \tag{7}$$

and, from (5), $e_{2i-1}^{k+1} + e_{2i}^{k+1} = 0$. Then, we can define $d_i^{k+1} = e_{2i-1}^{k+1}$. The algorithms for the direct (8) and inverse (9) transforms in the cell average framework are:

$\overline{f}^L \to M\overline{f}^L = \{\overline{f}^0, d^1, \ldots, d^L\}$ (Direct)

$$\begin{cases} \textbf{for } k = L-1,\ldots,0 \\ \quad \overline{f}_i^k = \frac{1}{2}(\overline{f}_{2i}^{k+1} + \overline{f}_{2i-1}^{k+1}), & 1 \le i \le N_k \\ \quad d_i^{k+1} = \overline{f}_{2i-1}^{k+1} - (P_k^{k+1}\overline{f}^k)_{2i-1}, & 1 \le i \le N_k \\ \textbf{end} \end{cases} \tag{8}$$

$M\overline{f}^L \to M^{-1}M\overline{f}^L$ (Inverse)

$$\begin{cases} \textbf{for } k = 0,\ldots,L-1 \\ \quad \overline{f}_{2i-1}^{k+1} = (P_k^{k+1}\overline{f}^k)_{2i-1} + d_i^{k+1}, & 1 \le i \le N_k \\ \quad \overline{f}_{2i}^{k+1} = 2\overline{f}_i^k - \overline{f}_{2i-1}^{k+1} \equiv (P_k^{k+1}\overline{f}^k)_{2i} - d_i^{k+1}, & 1 \le i \le N_k \\ \textbf{end} \end{cases} \tag{9}$$

3 *Interp-$\mathscr{LS}$* reconstruction for cell averages

3.1 *Interp-$\mathscr{LS}$ reconstruction for point values ($\overline{\mathscr{ILSP}}$)*

As in [12] the *Interp-$\mathscr{LS}$* reconstruction is defined as follows: Given k and the interval $I_i^k = [x_{i-1}^k, x_i^k]$ we construct the polynomial of degree r such that interpolates x_{i-1}^k, x_i^k and approximates in the sense of least squares at the $nl + nr > r - 1$ nodes x_{i+j}^k, $j = -nl,\ldots,-2,1,\ldots,nr-1$. If we denote $q_{i,nl,nr}^{\overline{\mathscr{ILSP}}^r}(x;f^k)$ this polynomial, then the reconstruction is

$$\overline{\mathscr{ILSP}}^r_{nl,nr}(x;f^k) = q_{i,nl,nr}^{\overline{\mathscr{ILSP}}^r}(x;f^k),\ x \in [x_{i-1}^k, x_i^k]$$

and the prediction is

$$\left(P_k^{k+1}f^k\right)_{2i-1} = \overline{\mathscr{ILSP}}^r_{nl,nr}(x_{2i-1}^{k+1};f^k).$$

3.2 *Interp-$\mathscr{LS}$ reconstruction for cell averages ($\overline{\mathscr{ILSC}}$)*

Let $p_{i,nl,nr}^{\overline{\mathscr{ILSC}}^{r-1}}(x;\overline{f}^k) = \sum_{l=0}^{r-1}(l+1)a_l x^l$ the polynomial of degree $r-1 < n_l + n_r$, $(\in \Pi_{r-1})$ such that

$$\frac{1}{h_k}\int_{x_{i-1}^k}^{x_i^k} p_{i,nl,nr}^{\overline{\mathscr{ILSC}}^{r-1}}(x;\overline{f}^k)dx = \overline{f}_i^k \tag{10}$$

and

$$\frac{1}{h_k}\int_{x_{i+s-1}^k}^{x_{i+s}^k} p_{i,nl,nr}^{\overline{\mathscr{ILSC}}^{r-1}}(x)dx \approx \overline{f}_{i+s}^k,\ s = -nl,\ldots,nr,\ s \ne 0, \tag{11}$$

$nr, nl \in \mathbf{N}$, in the least square sense. That is, that minimizes

$$\min_{p_i(x)\in\Pi_{r-1}} \left|\left|\left(\frac{1}{h_k}\int_{x_{i+s-1}^k}^{x_{i+s}^k} p_i(x)dx - \overline{f}_{i+s}^k\right)_{s=-nl,\ldots,nr,\ s\ne 0}\right|\right|_2.$$

If we define $q_i(x) = \int_0^x p_{i,nl,nr}^{\overline{\mathscr{ILSC}}^{r-1}}(y;\overline{f}^k)dy = \sum_{l=0}^{r-1} a_l x^{l+1}$ and we assume, without loss of generality, that $i = 0$ and $x_{i+s-1}^k = s$, then (10) is equivalent to

$$\frac{q_0(1) - q_0(0)}{1} = \sum_{l=0}^{r-1} a_l = \overline{f}_0^k.$$

Since $a_0 = \overline{f}_0^k - \sum_{l=1}^{r-1} a_l$, then

$$q_0(x) = (\overline{f}_0^k - \sum_{l=1}^{r-1} a_l)x + \sum_{l=1}^{r-1} a_l x^{l+1} = x\overline{f}_0^k + \sum_{l=1}^{r-1} a_l(x^{l+1} - x).$$

Conditions (11) are equivalent to

$$\frac{q_0(s+1) - q_0(s)}{1} = \overline{f}_0^k + \sum_{l=1}^{r-1} a_l\left((s+1)^{l+1} - s^{l+1} - 1\right) \approx \overline{f}_s^k \tag{12}$$

in the least square sense and

$$\sum_{l=1}^{r-1} a_l\left((s+1)^{l+1} - s^{l+1} - 1\right) \approx \overline{f}_s^k - \overline{f}_0^k,\ s = -nl,\ldots,nr,\ s \ne 0.$$

Then we have to obtain $\hat{a} \in \mathbf{R}^{r-1}$ such that minimizes

$$\min_{\hat{a}\in\mathbf{R}^{r-1}} \left|\left|A_{nl,nr}^{\overline{\mathscr{ILSC}}^{r-1}}\hat{a} - \left(\hat{f} - \mathbf{1}_{\mathbf{nl+nr}}\overline{f}_0\right)\right|\right|_2,$$

where:

$$A_{nl,nr}^{\overline{\mathscr{ILSC}}^{r-1}} = \begin{bmatrix} (-nl+1)^2 - (-nl)^2 - 1 & \cdots & (-nl+1)^r - (-nl)^r - 1 \\ \vdots & \ddots & \vdots \\ -(-1)^2 - 1 & \cdots & -(-1)^r - 1 \\ 2^2 - 1^2 - 1 & \cdots & 2^r - 1^r - 1 \\ \vdots & \ddots & \vdots \\ (nr+1)^2 - (nr)^2 - 1 & \cdots & (nr+1)^r - (nr)^r - 1 \end{bmatrix}, \tag{13}$$

© 2016 NSP
Natural Sciences Publishing Cor.

$\hat{a} = [a_1, \ldots, a_{r-1}]^T$, $\hat{f} = [\overline{f}^k_{-nl}, \ldots, \overline{f}^k_{-1}, \overline{f}^k_1, \ldots, \overline{f}^k_{nr}]^T$ and $\mathbf{1_n} = (\underbrace{1, \ldots, 1}_{n})^T$.

Then, using the normal equations,

$$\hat{a} = \left(A^{\overline{\mathscr{ILSC}}^{r-1}T}_{nl,nr} A^{\overline{\mathscr{ILSC}}^{r-1}}_{nl,nr} \right)^{-1} A^{\overline{\mathscr{ILSC}}^{r-1}T}_{nl,nr} (\hat{f} - \mathbf{1_{nl+nr}}\,\overline{f}_0),$$

$$a_0 = \overline{f}_0 - \mathbf{1_{r-1}}^T \hat{a}.$$

Once we have $\{a_l\}_{l=0}^{r-1}$ and $p^{\overline{\mathscr{ILSC}}^{r-1}}_{i,nl,nr}(x; \overline{f}^k)$ we define the reconstruction as

$$\overline{\mathscr{ILSC}}^{r-1}_{nl,nr}(x; \overline{f}^k) = p^{\overline{\mathscr{ILSC}}^{r-1}}_{i,nl,nr}(x; \overline{f}^k),\ x \in [x^k_{i-1}, x^k_i], \tag{14}$$

and the prediction

$$\begin{aligned}
\left(P^{k+1}_k \overline{f}^k\right)_{2i-1} &= \frac{1}{h_{k+1}} \int_{x^{k+1}_{2i-2}}^{x^{k+1}_{2i-1}} \overline{\mathscr{ILSC}}^{r-1}_{nl,nr}(x; \overline{f}^k) dx \\
&= \sum_{l=-nl}^{nr} (\gamma^r_{nl,nr})_l\, \overline{f}^k_{i+l}, \\
\left(P^{k+1}_k \overline{f}^k\right)_{2i} &= \frac{1}{h_{k+1}} \int_{x^{k+1}_{2i}}^{x^{k+1}_{2i-1}} \overline{\mathscr{ILSC}}^{r-1}_{nl,nr}(x; \overline{f}^k) dx \\
&\equiv 2\overline{f}^k_i - \left(P^{k+1}_k \overline{f}^k\right)_{2i-1}.
\end{aligned}$$

Table 1: Filters, $(\gamma^r_{nl,nr})_l$, of the approximations to $\overline{f}^{k+1}_{2i-1}$ obtained with the $\overline{\mathscr{ILSC}}^{r-1}_{nl,nr}$ reconstruction $\left(P^{k+1}_k \overline{f}^k\right)_{2i-1} = \sum_{l=-nl}^{nr} (\gamma^r_{nl,nr})_l\, \overline{f}^k_{i+l}$.

l	-4	-3	-2	-1	0	1	2	3	4
$(\gamma^2_{2,0})_l$			$\frac{2}{20}$	$\frac{1}{20}$	$\frac{17}{20}$				
$(\gamma^2_{3,0})_l$		$\frac{3}{56}$	$\frac{2}{56}$	$\frac{1}{56}$	$\frac{50}{56}$				
$(\gamma^2_{4,0})_l$	$\frac{4}{120}$	$\frac{3}{120}$	$\frac{2}{120}$	$\frac{1}{120}$	$\frac{110}{120}$				
$(\gamma^2_{0,2})_l$					$\frac{23}{20}$	$-\frac{1}{20}$	$-\frac{2}{20}$		
$(\gamma^2_{0,3})_l$					$\frac{62}{56}$	$-\frac{1}{56}$	$-\frac{2}{56}$	$-\frac{3}{56}$	
$(\gamma^2_{0,4})_l$					$\frac{130}{120}$	$-\frac{1}{120}$	$-\frac{2}{120}$	$-\frac{3}{120}$	$-\frac{4}{120}$
$(\gamma^3_{2,2})_l$			$\frac{2}{40}$	$\frac{1}{40}$	$\frac{40}{40}$	$-\frac{1}{40}$	$-\frac{2}{40}$		
$(\gamma^3_{3,3})_l$		$\frac{3}{112}$	$\frac{2}{112}$	$\frac{1}{112}$	$\frac{112}{112}$	$-\frac{1}{112}$	$-\frac{2}{112}$	$-\frac{3}{112}$	
$(\gamma^3_{4,4})_l$	$\frac{4}{240}$	$\frac{3}{240}$	$\frac{2}{240}$	$\frac{1}{240}$	$\frac{240}{240}$	$-\frac{1}{240}$	$-\frac{2}{240}$	$-\frac{3}{240}$	$-\frac{4}{240}$

In Table 1, we show the filters, $(\gamma^r_{nl,nr})_l$, for different degrees of the polynomial, r, and different sizes of stencil.

As in [12] and [2] we can prove the following results:

Proposition 1. *The matrix $A^{\overline{\mathscr{ILSC}}^{r-1}}_{nl,nr}$, $r > 1$, $nl + nr > r - 1$, defined in (13), has full rank.*

Proof. We will prove that $A^{\overline{\mathscr{ILSC}}^{r-1}}_{nl,nr}$ has full rank, i.e $rank(A^{\overline{\mathscr{ILSC}}^{r-1}}_{nl,nr}) = r - 1$, by induction on the degree of the polynomial $p^{\overline{\mathscr{ILSC}}^{r-1}}_{nl,nr}$.

When $r = 2$ we have a single vector, so the rank is 1. Let $r \in \mathbf{N}$, $r > 2$, and assume that $rank(A^{\overline{\mathscr{ILSC}}^{r-1}}_{nl,nr}) = r - 1$. We want to see whether $rank(A^{\overline{\mathscr{ILSC}}^{r}}_{nl+a,nr+b}) = r$, $nl + a + nl + b > r$, $a \geq 0$, $b \geq 0$, $a \in \mathbf{N}$, $b \in \mathbf{N}$.

Since $rank(A^{\overline{\mathscr{ILSC}}^{r-1}}_{nl,nr}) = r - 1$, there is a submatrix M_{r-1} of $A^{\overline{\mathscr{ILSC}}^{r-1}}_{nl,nr}$ such that $|M_{r-1}| \neq 0$.

Without loss of generality, we suppose that $nl \geq 1$, $a = 1, b = 0$ (otherwise we could use the last row and apply the same reasoning). Then

$$A^{\overline{\mathscr{ILSC}}^{r}}_{nl+1,nr} = \left[\begin{array}{c|c} \frac{(-nl)^2 - (-nl-1)^2 - 1 \cdots}{A^{\overline{\mathscr{ILSC}}^{r-1}}_{nl,nr}} & \begin{array}{c} (-nl)^{r+1} - (-nl-1)^{r+1} - 1 \\ \vdots \\ (nr+1)^{r+1} - nr^{r+1} - 1 \end{array} \end{array}\right].$$

Given that $nl \geq 1$ and $r \geq 2$:

$$\begin{aligned}
(-nl)^{r+1} - (-nl-1)^{r+1} - 1 &= (-1)^{r+2}\left(\sum_{k=1}^{r+1} \binom{r+1}{k} nl^{r+1-k}\right) - 1 \\
&\neq 0.
\end{aligned} \tag{15}$$

Then, $(-nl)^{r+1} - (-nl-1)^{r-1} - 1$ can be used as the pivot element to nullify the elements of its column. If we denote N_{r-1} as the result of applying to M_{r-1} the linear transformations that enable nullify such elements, we can define the $r \times r$ matrix:

$$A_r = \left[\begin{array}{c|c} a'_1 \cdots a'_{r-1} & \begin{array}{c} (-nl)^{r+1} - (-nl-1)^{r+1} - 1 \\ 0 \end{array} \\ \hline N_{r-1} & \begin{array}{c} \vdots \\ 0 \end{array} \end{array}\right],$$

where its first row elements $a'_{1,j} \in A_r$ are $a'_{1,j} = a_{1,j} \in A^{\overline{\mathscr{ILSC}}^{r}}_{nl+1,nr}$, such that $a_{i,j} \in M_{r-1}$. Therefore, by (15) and the induction hypothesis,

$$\begin{aligned}
|A_r| &= (-1)^{r+1}\left((-nl)^{r+1} - (-nl-1)^{r-1} - 1\right)|N_r| \\
&= (-1)^{r+1}\left((-nl)^{r+1} - (-nl-1)^{r-1} - 1\right)|M_r| \neq 0,
\end{aligned}$$

and then, $rank(A^{\overline{\mathscr{ILSC}}^{r}}_{nl+1,nr}) = r$.

Finally, by the principle of induction we have the result.

Proposition 2. *The Interp-$\mathscr{LS}$ reconstruction for cell averages has a unique solution.*

Proof. Since the matrix $A^{\overline{\mathscr{ILSC}}^{r-1}}_{nl,nr}$, defined in (13), has full rank by Proposition 1, following section 3.2, the *Interp-$\mathscr{LS}$* reconstruction for cell averages has a unique solution.

Proposition 3. *If $p^{\overline{\mathscr{ILSC}}^{r-1}}_{i,nl,nr}(x; \overline{f}^k)$ is the polynomial $\overline{\mathscr{ILSC}}$ of degree $r - 1$, the Interp-$\mathscr{LS}$ reconstruction for cell averages recovers exactly polynomials of degree s, $0 \leq s \leq r - 1$.*

© 2016 NSP
Natural Sciences Publishing Cor.

*Proof.*Let $p(x)=\sum_{l=0}^{s} b_l x^l$ be a polynomial of degree s, with $0\le s\le r-1$. We define $\{\bar{f}_j\}_{j=0}^{m}$, $m>r-1$, as:

$$\int_j^{j+1} p(x)=\bar{f}_j,\qquad j=0,\dots,m, \tag{16}$$

and

$$q(x)=\int_0^x p(x)=\sum_{l=0}^{s} a_l x^{l+1}, \tag{17}$$

where $a_l=\frac{b_l}{l+1}$, $l=0,\dots,s$.

Thanks to (16) we have that $A_{0,m}^{\overline{\mathscr{ILSC}}^s}\hat{a}=\hat{f}-\mathbf{1_{m-1}}\bar{f}_0$, where $\hat{a}=[a_1,\dots,a_s]^T$, $\hat{f}=[\bar{f}_1^k,\dots,\bar{f}_m^k]^T$ and $A_{0,m}^{\overline{\mathscr{ILSC}}^s}$ is defined in (13). Then

$$\left\|A_{0,m}^{\overline{\mathscr{ILSC}}^s}\hat{a}-(\hat{f}-\mathbf{1_{m-1}}\bar{f}_0)\right\|_2=0. \tag{18}$$

On the other hand, we know that the *Interp-*$\mathscr{LS}$ problem for cell averages has a unique solution by Proposition 2. In particular, whether

$$p_{i,0,m}^{\overline{\mathscr{ILSC}}^{r-1}}=\sum_{l=0}^{r-1}(l+1)a_l x^l$$

is the solution of the *Interp-*$\mathscr{LS}$ problem defined by (10) and (11), with $\{\bar{f}_j\}_{j=0}^{m}$, $m>r-1$, defined by (16), and since $q(x)$ is the solution of this problem by (18), we have that $p^{\overline{\mathscr{ILSC}}}=q(x)$, and therefore the *Interp-*$\mathscr{LS}$ reconstruction recovers exactly $q(x)$.

Corollary 1.*The order of the Interp-*$\mathscr{LS}$ *reconstruction for cell averages is r.*

3.3 Nonlinear Reconstructions for cell averages

When using the *Interp-*$\mathscr{LS}$ reconstruction for cell averages we have that if r increases, $r\le m=nr+nl+1$, the interpolation process has higher order accuracy, i.e. the details d_i^{k+1} will be smaller when f is smooth on $[x_{i-nl-1}^k,x_{i+nr}^k]$. On the other hand, the interval $[x_{i-nl-1}^k,x_{i+nr}^k]$ gets larger with nr,nl so that a singularity in (x_{i-1}^k,x_i^k) will affect more detail coefficients. Non-linear essentially non-oscillatory (*ENO*) interpolation techniques, which were firstly introduced in [9], circumvent this drawback.

3.3.1 *ENO Interp-*$\mathscr{LS}$ reconstruction for cell averages ($E\overline{\mathscr{ILSC}}$)

The idea of *ENO* interpolation technique is to replace in (14) the polynomial $p_{i,nl,nr}^{\overline{\mathscr{ILSC}}^{r-1}}(x;\bar{f}^k)$ by $p_{i,nl_i,m-nl_i}^{\overline{\mathscr{ILSC}}^{r-1}}(x;\bar{f}^k)$ selected among the $m+1$ polynomials $\{p_{i,s,m-s}^{\overline{\mathscr{ILSC}}^{r-1}}(x;\bar{f}^k)\}_{s=0}^{m}$, where $m=nr+nl+1$, in order to avoid the influence of the singularity. In [2,8,9] the selection process is made by picking the "least oscillatory" polynomial using numerical information on the divided differences of f at the points x_l^k. That is, using the stencil that minimizes $f[x_{i-l}^k,\dots,x_{i+m-l-1}^k]$, $1\le l\le m-1$.

Here, inspired by [11], we use a selection which gives us better results in the presence of noise. First, we define

$$E_2(i,s,m)=\sum_{l=0}^{m-1}\left(\frac{1}{h_k}\int_{x_{i-s+l-1}^k}^{x_{i-s+l}^k} p_{i,s,m-1-s}^{\overline{\mathscr{ILSC}}^{r-1}}(x,\bar{f}^k)dx-\bar{f}_{i-s+l}^k\right)^2 \tag{19}$$

and now

$$E_2(i,nl_i,m)=min_{s=0,\dots,m-1}\{E_2(i,s,m)\}. \tag{20}$$

Once this selection is made, we thus define

$$E\overline{\mathscr{ILSC}}_{nl,nr}^{r-1}(x;\bar{f}^k)=p_{i,nl_i,m-1-nl_i}^{\overline{\mathscr{ILSC}}^{r-1}}(x;\bar{f}^k),\ x\in[x_{i-1}^k,x_i^k]$$

and

$$\left(P_k^{k+1}\bar{f}^k\right)_{2i-1}=\frac{1}{h_{k+1}}\int_{x_{2i-2}^{k+1}}^{x_{2i-1}^{k+1}} E\overline{\mathscr{ILSC}}_{nl,nr}^{r-1}(x;\bar{f}^k)dx,$$

$$\left(P_k^{k+1}\bar{f}^k\right)_{2i}=2\bar{f}_i^k-\left(P_k^{k+1}\bar{f}^k\right)_{2i-1}.$$

3.3.2 *SR Interp-*$\mathscr{LS}$ reconstruction for cell averages ($S\overline{\mathscr{ILSC}}$)

The *ENO* interpolatory technique still produces large details d_i^{k+1} when a singularity is contained in the interval $[x_{i-1}^k,x_i^k]$. In order to reduce further the interpolation error, subcell resolution methods (*SR*) were introduced in [7]. Now let's see how we can apply the *SR* technique ([1,7]) in the *Interp-*$\mathscr{LS}$ reconstruction for cell averages:

Assume that $f(x)$ has a jump in $[x_{i-1}^k,x_i^k]$. Then the *primitive function* of $f(x)$, $F(x)=\int_0^x f(y)dy\in\mathscr{C}([0,1])$, has a corner (a discontinuity in the derivative) there.

Note that the sets $\{\bar{f}_i^k\}_{i=1}^{N_k}$ and $F^k=\{F_i^k\}_{i=0}^{N_k}$ are equivalents due to the relations $F_i^k=F(x_i^k)=\int_0^{x_i^k} f(y)dy=h_k\sum_{j=1}^{i}\bar{f}_j^k$ and $\bar{f}_j^k=\frac{F_j^k-F_{j-1}^k}{h_k}$.

Then, as in [2] or [12], we can use the function (21) to detect where the singularity is.

The steps to apply the *SR* technique in the *Interp-*$\mathscr{LS}$ reconstruction for cell averages are:

1.- Taking *stencils* with $m=nl+nr+1$ nodes, we calculate the *stencil ENO* as in the previous section.

2.- If $nl_{i-1}=m-1$ and $nl_{i+1}=0$ the *stencils* for the cells I_{i-1}^k and I_{i+1}^k are disjoint. We label the cell as *suspect* of containing a discontinuity.

© 2016 NSP
Natural Sciences Publishing Cor.

3.- For each suspicious cell we define the function

$$G_i^{\overline{\mathscr{ILSC}}}(x) = q_{i+1,0,m-1}^{\overline{\mathscr{ILSP}}^r}(x;F^k) - q_{i-1,m-1,0}^{\overline{\mathscr{ILSP}}^r}(x;F^k). \tag{21}$$

If $G_i^{\overline{\mathscr{ILSC}}}(x_{i-1}^k)\cdot G_i^{\overline{\mathscr{ILSC}}}(x_i^k) < 0$ we label the cell I_i^k as singular.

4.- If $G_i^{\overline{\mathscr{ILSC}}}(x_{i-1}^k)\cdot G_i^{\overline{\mathscr{ILSC}}}(x_{2i-1}^{k+1}) > 0$, the node x_{2i-1}^{k+1} lies to the left of the discontinuity. Then $\left(P_k^{k+1}\overline{f}^k\right)_{2i-1}$ is obtained as follows

$$\left(P_k^{k+1}\overline{f}^k\right)_{2i-1} = \frac{q_{i-1,m-1,0}^{\overline{\mathscr{ILSP}}^r}(x_{2i-1}^{k+1};F^k) - q_{i-1,m-1,0}^{\overline{\mathscr{ILSP}}^r}(x_{2i-2}^{k+1};F^k)}{h_{k+1}}$$
$$= \sum_{l=-nl-nr-1}^{-1}\left(\gamma_{nl+nr+1,-1}^r\right)_l \overline{f}_{i+l}^k, \tag{22}$$

$$\left(P_k^{k+1}\overline{f}^k\right)_{2i} = 2\overline{f}_i^{k+1} - \left(P_k^{k+1}\overline{f}^k\right)_{2i-1}, \tag{23}$$

where some of these coefficients are in Table 2.

Table 2: Filters, $(\gamma_{nl,nr}^r)_l$, of the approximations to f_{2i-1}^{k+1}, obtained with the $S\overline{\mathscr{ILSC}}^{r-1}_{nl+nr+1,-1}$ reconstruction $\left(P_k^{k+1}\overline{f}^k\right)_{2i-1} = \Sigma_{l=-nl-nr-1}^{-1}(\gamma_{nl+nr+1,-1}^r)_l\,\overline{f}_{i+l}^k$.

l	-7	-6	-5	-4	-3	-2	-1
$\left(\gamma_{3,-1}^2\right)_l$					$-\frac{3}{10}$	$-\frac{3}{20}$	$\frac{29}{20}$
$\left(\gamma_{5,-1}^2\right)_l$			$-\frac{1}{10}$	$-\frac{3}{40}$	$-\frac{1}{20}$	$-\frac{1}{40}$	$\frac{5}{4}$
$\left(\gamma_{5,-1}^3\right)_l$			$\frac{89}{310}$	$-\frac{273}{1240}$	$-\frac{271}{620}$	$-\frac{451}{1240}$	$\frac{215}{124}$
$\left(\gamma_{7,-1}^3\right)_l$	$\frac{81}{512}$	$-\frac{65}{3584}$	$-\frac{241}{1792}$	$-\frac{171}{896}$	$-\frac{671}{3584}$	$-\frac{443}{3584}$	$\frac{383}{256}$
$\left(\gamma_{5,-1}^4\right)_l$			$-\frac{971}{2208}$	$\frac{1194}{985}$	$-\frac{549}{1472}$	$-\frac{2113}{1123}$	$\frac{1318}{531}$
$\left(\gamma_{7,-1}^4\right)_l$	$-\frac{384}{1349}$	$\frac{511}{1275}$	$\frac{263}{821}$	$-\frac{357}{2497}$	$-\frac{454}{749}$	$-\frac{1913}{2788}$	$\frac{1663}{832}$

In the other case ($G_i^{\overline{\mathscr{ILSC}}}(x_{i-1}^k)\cdot G_i^{\overline{\mathscr{ILSC}}}(x_{2i-1}^{k+1}) < 0$), x_{2i-1}^{k+1} is located to the right of the discontinuity and

$$\left(P_k^{k+1}\overline{f}^k\right)_{2i} = \frac{q_{i+1,0,m-1}^{\overline{\mathscr{ILSP}}^r}(x_{2i}^{k+1};F^k) - q_{i+1,0,m-1}^{\overline{\mathscr{ILSP}}^r}(x_{2i-1}^{k+1};F^k)}{h_{k+1}},$$
$$= \sum_{l=1}^{nl+nr+1}\left(\beta_{-1,nl+nr+1}^r\right)_l f_{i+l}^{k+1}. \tag{24}$$

$$\left(P_k^{k+1}\overline{f}^k\right)_{2i-1} = 2\overline{f}_i^{k+1} - \left(P_k^{k+1}\overline{f}^k\right)_{2i}, \tag{25}$$

where $(\beta_{-1,nl+nr+1}^r)_l = (\gamma_{nl+nr+1,-1}^r)_{-l}$, $l = 1,\ldots,nl+nr+1$.

Remark.(23) can be calculated as: $\left(P_k^{k+1}\overline{f}^k\right)_{2i} = \frac{1}{h_{k+1}}(q_{i+1,0,m-1}^{\overline{\mathscr{ILSP}}^r}(x_{2i}^{k+1};F^k) - q_{i-1,m-1,0}^{\overline{\mathscr{ILSP}}^r}(x_{2i-1}^{k+1};F^k))$. We can use (23) because the reconstruction is consistent due to the interpolatory conditions:

$$\frac{\overline{f}_{2i-1}^k + \overline{f}_{2i}^k}{2} = \frac{\left(P_k^{k+1}\overline{f}^k\right)_{2i-1} + \left(P_k^{k+1}\overline{f}^k\right)_{2i}}{2h_{k+1}} = \frac{F_i^k + F_{i-1}^k}{h_k} = \overline{f}_i^k.$$

The same could be said for (25).

Thanks to the interpolatory conditions, $G_i^{\overline{\mathscr{ILSC}}}$ can be expressed in terms of $\{\overline{f}_i^k\}$ (see [12] for details). For instance, the filters of (21) for $nl+nr=4$ and $r=3$ are:

$$G_i^{\overline{\mathscr{ILSC}}}(x_{i-1}^k) = h_k(\overline{f}_i^k - \tfrac{63}{31}\overline{f}_{i+1}^k + \tfrac{81}{155}\overline{f}_{i+2}^k + \tfrac{97}{155}\overline{f}_{i+3}^k + \tfrac{48}{155}\overline{f}_{i+4}^k - \tfrac{66}{155}\overline{f}_{i+5}^k),$$

$$G_i^{\overline{\mathscr{ILSC}}}(x_{2i-1}^{k+1}) = h_k(-\tfrac{89}{620}\overline{f}_{i-5}^k + \tfrac{273}{2480}\overline{f}_{i-4}^k + \tfrac{271}{1240}\overline{f}_{i-3}^k + \tfrac{451}{2480}\overline{f}_{i-2}^k - \tfrac{215}{248}\overline{f}_{i-1}^k + \overline{f}_i^k - \tfrac{215}{248}\overline{f}_{i+1}^k + \tfrac{451}{2480}\overline{f}_{i+2}^k + \tfrac{271}{1240}\overline{f}_{i+3}^k + \tfrac{273}{2480}\overline{f}_{i+4}^k - \tfrac{89}{620}\overline{f}_{i+5}^k),$$

$$G_i^{\overline{\mathscr{ILSC}}}(x_i^k) = h_k(-\tfrac{66}{155}\overline{f}_{i-5}^k + \tfrac{48}{155}\overline{f}_{i-4}^k + \tfrac{97}{155}\overline{f}_{i-3}^k + \tfrac{81}{155}\overline{f}_{i-2}^k - \tfrac{63}{31}\overline{f}_{i-1}^k + \overline{f}_i^k).$$

4 Least squares reconstruction for cell averages ($\overline{\mathscr{LSC}}$)

Let $p_{i,nl,nr}^{\overline{\mathscr{LSC}}^{r-1}}(x;\overline{f}^k) = \Sigma_{l=0}^{r-1}(l+1)a_l x^l$ the polynomial of the degree $r-1$ such that

$$\frac{1}{h_k}\int_{x_{i+s-1}^k}^{x_{i+s}^k} p_{i,nl,nr}^{\overline{\mathscr{LSC}}^{r-1}}(x;\overline{f}^k)dx \approx \overline{f}_{i+s}^k,\ \ s=-nl,\ldots,nr, \tag{26}$$

in the least square sense.

If we define $q_i(x) = \int_0^x p_{i,nl,nr}^{\overline{\mathscr{LSC}}^{r-1}}(y;\overline{f}^k)dy = \sum_{l=0}^{r-1}a_l x^{l+1}$ and we assume, without loss of generality, that $i=0$ and $x_{i+s-1}^k = s$, then (26) is equivalent to

$$\frac{q_0(s+1)-q_0(s)}{1} = \sum_{l=0}^{r-1}a_l\left((s+1)^{l+1}-s^{l+1}\right) \approx \overline{f}_s^k \tag{27}$$

and

$$\sum_{l=0}^{r-1}a_l\left((s+1)^{l+1}-s^{l+1}\right) \approx \overline{f}_s^k,\ \ s=-nl,\ldots,nr.$$

Then we have to obtain $\hat{a}\in\mathbf{R}^r$ that minimizes

$$\min_{\hat{a}\in\mathbf{R}^r}\left|\left|A_{nl,nr}^{\overline{\mathscr{LSC}}^{r-1}}\hat{a}-\hat{f}\right|\right|_2,$$

where:

$$A_{nl,nr}^{\overline{\mathscr{LSC}}^{r-1}} = \begin{bmatrix} (-nl+1)^1-(-nl)^1 & \cdots & (-nl+1)^r-(-nl)^r \\ \vdots & \ddots & \vdots \\ (nr+1)^1-(nr)^1 & \cdots & (nr+1)^r-(nr)^r \end{bmatrix} \tag{28}$$

© 2016 NSP
Natural Sciences Publishing Cor.

with $\hat{a} = [a_0, \ldots, a_{r-1}]^T$ and $\hat{f} = \left[\overline{f}^k_{-nl}, \ldots, \overline{f}^k_{nr}\right]^T$.

Then, using the normal equations,

$$\hat{a} = \left(A^{\overline{\mathscr{L}\mathscr{I}\mathscr{C}}^{r-1}T}_{nl,nr} A^{\overline{\mathscr{L}\mathscr{I}\mathscr{C}}^{r-1}}_{nl,nr} \right)^{-1} A^{\overline{\mathscr{L}\mathscr{I}\mathscr{C}}^{r-1}T}_{nl,nr} \hat{f}.$$

Once we have $\{a_l\}_{l=0}^{r-1}$ and $p^{\overline{\mathscr{L}\mathscr{I}\mathscr{C}}^{r-1}}_{i,nl,nr}(x;\overline{f}^k)$ we define the reconstruction

$$\overline{\mathscr{L}\mathscr{I}\mathscr{C}}^{r-1}_{nl,nr}(x;\overline{f}^k) = \int_{x^k_{i+s-1}}^{x^k_{i+s}} p^{\overline{\mathscr{L}\mathscr{I}\mathscr{C}}^{r-1}}_{i,nl,nr}(x;\overline{f}^k)dx,\ x \in [x^k_{i-1}, x^k_i],$$

and the prediction

$$\begin{aligned}\left(P^{k+1}_k \overline{f}^k\right)_{2i-1} &= \frac{1}{h_{k+1}} \int_{x^{k+1}_{2i-2}}^{x^{k+1}_{2i-1}} \overline{\mathscr{L}\mathscr{I}\mathscr{C}}^{r-1}_{nl,nr}(x;\overline{f}^k)dx \\ &= \sum_{l=-nl}^{nr} (\gamma^r_{nl,nr})_l \overline{f}^k_{i+l}, \qquad (29)\\ \left(P^{k+1}_k \overline{f}^k\right)_{2i} &= \frac{1}{h_{k+1}} \int_{x^{k+1}_{2i-1}}^{x^{k+1}_{2i}} \overline{\mathscr{L}\mathscr{I}\mathscr{C}}^{r-1}_{nl,nr}(x;\overline{f}^k)dx \\ &= \sum_{l=-nl}^{nr} (\beta^r_{nl,nr})_l \overline{f}^k_{i+l}. \qquad (30)\end{aligned}$$

In Table 3 and 4 we can see some of these coefficients.

Table 3: Filters, $(\gamma^r_{nl,nr})_l$, of the approximations to $\overline{f}^{k+1}_{2i-1}$ obtained with the $\overline{\mathscr{L}\mathscr{I}\mathscr{C}}^{r-1}_{nl,nr}$ reconstruction, $\left(P^{k+1}_k \overline{f}^k\right)_{2i-1} = \sum_{l=-nl}^{nr} (\gamma^r_{nl,nr})_l \overline{f}^k_{i+l}$.

l	-4	-3	-2	-1	0	1	2	3	4
$(\gamma^2_{2,0})_l$			$\frac{-1}{14}$	$\frac{1}{3}$	$\frac{17}{24}$				
$(\gamma^2_{1,1})_l$				$\frac{11}{24}$	$\frac{1}{3}$	$\frac{5}{24}$			
$(\gamma^2_{0,2})_l$					$\frac{23}{24}$	$\frac{1}{3}$	$\frac{-7}{24}$		
$(\gamma^3_{4,0})_l$	$\frac{-1}{140}$	$\frac{-13}{280}$	$\frac{2}{35}$	$\frac{17}{56}$	$\frac{97}{140}$				
$(\gamma^3_{3,1})_l$		$\frac{-23}{140}$	$\frac{13}{56}$	$\frac{29}{70}$	$\frac{107}{280}$	$\frac{19}{140}$			
$(\gamma^3_{2,2})_l$			$\frac{-1}{28}$	$\frac{103}{280}$	$\frac{17}{35}$	$\frac{89}{280}$	$\frac{-19}{140}$		
$(\gamma^3_{1,3})_l$				$\frac{53}{140}$	$\frac{101}{280}$	$\frac{19}{70}$	$\frac{31}{280}$	$\frac{-17}{140}$	
$(\gamma^3_{0,4})_l$					$\frac{151}{140}$	$\frac{59}{280}$	$\frac{-8}{35}$	$\frac{-67}{280}$	$\frac{5}{28}$
$(\gamma^4_{3,3})_l$		$\frac{-315}{2688}$	$\frac{565}{2688}$	$\frac{925}{2688}$	$\frac{1}{3}$	$\frac{616}{2688}$	$\frac{29}{384}$	$\frac{-65}{896}$	
$(\gamma^4_{4,4})_l$	$\frac{-7}{64}$	$\frac{383}{4224}$	$\frac{553}{2636}$	$\frac{1257}{4825}$	$\frac{59}{231}$	$\frac{242}{1169}$	$\frac{784}{6131}$	$\frac{43}{1408}$	$\frac{-51}{704}$

Is well known by the least squares problem, that the matrix $A^{\overline{\mathscr{L}\mathscr{I}\mathscr{C}}^{r-1}}_{nl,nr}$, defined in (28), has full rank. Therefore, similarly to Proposition 3 we can prove the results:

Proposition 4. *If $p^{\overline{\mathscr{L}\mathscr{I}\mathscr{C}}^{r-1}}_{i,nl,nr}(x;f)$ is the polynomial $\overline{\mathscr{L}\mathscr{I}\mathscr{C}}$ of degree $r-1$, the $\mathscr{L}\mathscr{I}$ reconstruction for cell averages recovers exactly polynomials of degree s, $0 \le s \le r-1$.*

Corollary 2. *The order of the $\mathscr{L}\mathscr{I}$ reconstruction for cell averages is r.*

Table 4: Filters, $(\beta^r_{nl,nr})_l$, of the approximations to $\overline{f}^{k+1}_{2i}$ obtained with the $\overline{\mathscr{L}\mathscr{I}\mathscr{C}}^{r-1}_{nl,nr}$ reconstruction, $(P^{k+1}_k \overline{f}^k)_{2i} = \sum_{l=-nl}^{nr} (\beta^r_{nl,nr})_l \overline{f}^k_{i+l}$.

l	-4	-3	-2	-1	0	1	2	3	4
$(\beta^2_{2,0})_l$			$\frac{-7}{24}$	$\frac{1}{3}$	$\frac{23}{24}$				
$(\beta^2_{1,1})_l$				$\frac{5}{24}$	$\frac{1}{3}$	$\frac{11}{24}$			
$(\beta^2_{0,2})_l$					$\frac{17}{24}$	$\frac{1}{3}$	$\frac{-1}{24}$		
$(\beta^3_{4,0})_l$	$\frac{5}{28}$	$\frac{-67}{280}$	$\frac{-8}{35}$	$\frac{59}{280}$	$\frac{151}{140}$				
$(\beta^3_{3,1})_l$		$\frac{-17}{140}$	$\frac{31}{280}$	$\frac{19}{70}$	$\frac{101}{280}$	$\frac{53}{140}$			
$(\beta^3_{2,2})_l$			$\frac{-19}{140}$	$\frac{89}{280}$	$\frac{17}{35}$	$\frac{103}{280}$	$\frac{-1}{28}$		
$(\beta^3_{1,3})_l$				$\frac{19}{140}$	$\frac{107}{280}$	$\frac{29}{70}$	$\frac{13}{56}$	$\frac{-23}{140}$	
$(\beta^3_{0,4})_l$					$\frac{97}{140}$	$\frac{17}{56}$	$\frac{2}{35}$	$\frac{-13}{280}$	$\frac{-1}{140}$
$(\beta^4_{3,3})_l$		$\frac{-65}{896}$	$\frac{29}{384}$	$\frac{611}{2688}$	$\frac{1}{3}$	$\frac{925}{2688}$	$\frac{565}{2698}$	$\frac{-317}{2688}$	
$(\beta^4_{4,4})_l$	$\frac{-51}{704}$	$\frac{43}{1408}$	$\frac{784}{6131}$	$\frac{242}{1169}$	$\frac{59}{231}$	$\frac{1257}{4825}$	$\frac{553}{2636}$	$\frac{383}{4224}$	$\frac{-7}{64}$

Observe that, since $\frac{1}{h_k}\int_{x^k_{i-1}}^{x^k_i} p_i(x)dx \neq \overline{f}^k_i$, this reconstruction do not satisfy (1) and (3). Then (7) is not true and $2\overline{f}^k_i - \overline{f}^{k+1}_{2i-1} \neq (P^{k+1}_k \overline{f}^k)_{2i} - d^{k+1}_i$.

Then, if we define, in (9), $\overline{f}^{k+1}_{2i} = (P^{k+1}_k \overline{f}^k)_{2i} - d^{k+1}_i$, the inverse transform is

$M\overline{f}^L \to M^{-1}M\overline{f}^L$

$$\begin{cases} \textbf{for } k & = 0, \ldots, L-1 \\ \quad \overline{f}^{k+1}_{2i-1} & = (P^{k+1}_k \overline{f}^k)_{2i-1} + d^{k+1}_i, \ 1 \le i \le N_k \\ \quad \overline{f}^{k+1}_{2i} & = (P^{k+1}_k \overline{f}^k)_{2i} - d^{k+1}_i, \quad 1 \le i \le N_k \\ \textbf{end} \end{cases} \qquad (31)$$

and the reconstruction is not consistent. We call it $\overline{\mathscr{L}\mathscr{I}\mathscr{C} - NC}$. To ensure the consistency we can use $\overline{f}^{k+1}_{2i} = 2\overline{f}^k_i - \overline{f}^{k+1}_{2i-1}$. In this case the inverse transform is:

$M\overline{f}^L \to M^{-1}M\overline{f}^L$

$$\begin{cases} \textbf{for } k & = 0, \ldots, L-1 \\ \quad \overline{f}^{k+1}_{2i-1} & = (P^{k+1}_k \overline{f}^k)_{2i-1} + d^{k+1}_i, \ 1 \le i \le N_k \\ \quad \overline{f}^{k+1}_{2i} & = 2\overline{f}^k_i - \overline{f}^{k+1}_{2i-1}, \quad 1 \le i \le N_k \\ \textbf{end} \end{cases} \qquad (32)$$

and we call it $\overline{\mathscr{L}\mathscr{I}\mathscr{C}}$.

4.1 ENO and SR $\mathscr{L}\mathscr{I}$ reconstruction for cell averages ($E\overline{\mathscr{L}\mathscr{I}\mathscr{C}}$ and $S\overline{\mathscr{L}\mathscr{I}\mathscr{C}}$)

While *ENO* can be applied as in section 3.3.1 (obtaining the $E\overline{\mathscr{L}\mathscr{I}\mathscr{C}}$ reconstruction), we have a problem applying *SR* in this case. The fact that we do not have the consistency implies that we do not know the point values of the primitive function (as in Section 3.3.2) and then we can not locate where the discontinuity is.

A way to apply the *SR* in this context is using the function $G^{\overline{\mathscr{I}\mathscr{L}\mathscr{I}\mathscr{C}}}_i(x)$ (21) to detect the singularity (as in

© 2016 NSP
Natural Sciences Publishing Cor.

section 3.3.2) and then, if the jump is in $[x_{2i-1}^{k+1}, x_{2i}^{k+1}]$, we evaluate (29)

$$\left(P_k^{k+1}\bar{f}^k\right)_{2i-1} = \frac{1}{h_{k+1}}\int_{x_{2i-2}^{k+1}}^{x_{2i-1}^{k+1}} \overline{\mathscr{LSC}}^{r-1}_{nl+nr+1,-1}(x;\bar{f}^k)dx$$
$$= \sum_{l=-nl-nr-1}^{-1} \left(\gamma^r_{nl+nr+1,-1}\right)_l \bar{f}^k_{i+l}, \qquad (33)$$

$$\left(P_k^{k+1}\bar{f}^k\right)_{2i} = 2\bar{f}_i^{k+1} - \left(P_k^{k+1}\bar{f}^k\right)_{2i-1}, \qquad (34)$$

and in the other case (30)

$$\left(P_k^{k+1}\bar{f}^k\right)_{2i} = \frac{1}{h_{k+1}}\int_{x_{2i-1}^{k+1}}^{x_{2i}^{k+1}} \overline{\mathscr{LSC}}^{r-1}_{-1,nl+nr+1,}(x;\bar{f}^k)dx \qquad (35)$$
$$= \sum_{l=1}^{nl+nr+1} \left(\beta^r_{-1,nl+nr+1}\right)_l f_{i+l}^{k+1},$$

$$\left(P_k^{k+1}\bar{f}^k\right)_{2i-1} = 2\bar{f}_i^{k+1} - \left(P_k^{k+1}\bar{f}^k\right)_{2i}. \qquad (36)$$

In Table 5 we show some of the coefficients β and $(\gamma^r_{nl+nr+1,-1})_{-l} = (\beta^r_{-1,nl+nr+1})_l$, $l = 1,\ldots,nl+nr+1$.

We call this reconstruction $S\overline{\mathscr{LSC}}$. Notice that it is consistent because we force it by (34) and (36).

We also can set a non consistent reconstruction as in (31), denoted by $S\overline{\mathscr{LSC}-NC}$ and defined as $S\overline{\mathscr{LSC}}$ but introducing the following changes:

–Replacing (34) by:

$$\left(P_k^{k+1}\bar{f}^k\right)_{2i} = (p^{\overline{\mathscr{LSP}}^r}_{i,-1,nl+nr+1}(x_{2i}^{k+1};F^k)$$
$$-p^{\overline{\mathscr{LSP}}^r}_{i,nl+nr+1,-1}(x_{2i-1}^{k+1};F^k))/(h_{k+1}), \qquad (37)$$

–and replacing (36) by:

$$\left(P_k^{k+1}\bar{f}^k\right)_{2i-1} = (p^{\overline{\mathscr{LSP}}^r}_{i,-1,nl+nr+1}(x_{2i-1}^{k+1};F^k)$$
$$-p^{\overline{\mathscr{LSP}}^r}_{i,nl+nr+1,-1}(x_{2i-2}^{k+1};F^k))/(h_{k+1}) \qquad (38)$$

where $p^{\overline{\mathscr{LSP}}^r}_{i,nl,nr}(x;F^k)$ denotes the $\mathscr{LS}$ reconstruction for point values. Its definition is the same as in the $\overline{\mathscr{ILSP}}$ reconstruction (section 3.1) but here the polynomial approximates in the sense of least squares at the $m > r+1$ nodes x_{i+j}^k, $j = -nl,\ldots,nr-1$ (see [12] for details).

4.2 Combining $S\overline{\mathscr{ILSC}}$ and $S\overline{\mathscr{LSC}}$

Consistent reconstructions recover properly the jumps but with non consistent reconstructions the exact location of them is lost. On the other hand, $S\overline{\mathscr{LSC}-NC}$ is expected to produce smoother results than $S\overline{\mathscr{LSC}}$, because (34) and (36) will produce oscillations in the solutions. In order to take advantage of both schemes we create a combined algorithm between $S\overline{\mathscr{ILSC}}$ and $S\overline{\mathscr{LSC}-NC}$ denoted as $S\overline{\mathscr{ILSC}-\mathscr{LSC}}$. The idea is through the algorithm of $S\overline{\mathscr{ILSC}}$ introduce a second function that calculates the $S\overline{\mathscr{LSC}-NC}$ reconstruction.

Table 5: Filters, $(\beta^r_{-1,nl+nr+1})_l$, of the approximations to f_{2i}^{k+1} obtained with the $S\overline{\mathscr{LSC}}^{r-1}_{-1,nl+nr+1}$ reconstruction. $\left(P_k^{k+1}\bar{f}^k\right)_{2i} = \sum_{l=1}^{nl+nr+1}(\beta^r_{-1,nl+nr+1})_l \bar{f}^k_{i+l}$.

l	1	2	3	4	5	6	7
$\left(\beta^2_{-1,4}\right)$	$\frac{37}{40}$	$\frac{19}{40}$	$\frac{1}{40}$	$-\frac{17}{40}$			
$\left(\beta^3_{-1,5}\right)$	$\frac{43}{28}$	$\frac{23}{240}$	$-\frac{41}{70}$	$-\frac{131}{280}$	$\frac{61}{140}$		
$\left(\beta^4_{-1,6}\right)$	$\frac{2394}{1135}$	$-\frac{6547}{8064}$	$-\frac{1861}{2016}$	$\frac{349}{2016}$	$\frac{529}{605}$	$-\frac{159}{377}$	
$\left(\beta^4_{-1,7}\right)$	$\frac{1663}{898}$	$-\frac{478}{1565}$	$-\frac{501}{629}$	$-\frac{1}{3}$	$-\frac{514}{1397}$	$\frac{227}{384}$	$-\frac{1021}{2688}$

The *SR* decision will be done by the $S\overline{\mathscr{ILSC}}$ scheme, avoiding losing the location of jumps but enabling a least squares approximation both in $\bar{f}_{2i-1}^k$ and $\bar{f}_{2i}^k$.

To sum up, initially we set $\{f_i^L\}_{i=1}^{N_L} = \{g_i^L\}_{i=1}^{N_L}$, and introduce the $S\overline{\mathscr{LSC}}$ reconstruction in the $S\overline{\mathscr{ILSC}}$ *SR* loop: The function $G_i^{\overline{\mathscr{ILSC}}}(x)$ (21) is used to detect the singularity (as in section 3.3.2) and then, if the jump is in $[x_{2i-1}^{k+1}, x_{2i}^{k+1}]$, we calculate:

$$\begin{cases} \left(P_k^{k+1}\bar{f}^k\right)_{2i-1} \text{ as in (22)}, \\ \left(P_k^{k+1}\bar{f}^k\right)_{2i} = 2\bar{f}_i^{k+1} - \left(P_k^{k+1}\bar{f}^k\right)_{2i-1}, \\ \left(P_k^{k+1}\bar{g}^k\right)_{2i-1} \text{ as in (33) substituting } \bar{f} \text{ by } \bar{g}, \\ \left(P_k^{k+1}\bar{g}^k\right)_{2i} \text{ as in (37) replacing } \bar{f} \text{ by } \bar{g}. \end{cases} \qquad (39)$$

In the other case the jump is in $[x_{2i-2}^{k+1}, x_{2i-1}^{k+1}]$ and:

$$\begin{cases} \left(P_k^{k+1}\bar{f}^k\right)_{2i} \text{ as in (24)}, \\ \left(P_k^{k+1}\bar{f}^k\right)_{2i-1} = 2\bar{f}_i^{k+1} - \left(P_k^{k+1}\bar{f}^k\right)_{2i}, \\ \left(P_k^{k+1}\bar{g}^k\right)_{2i} \text{ as in (35) substituting } \bar{f} \text{ by } \bar{g}, \\ \left(P_k^{k+1}\bar{g}^k\right)_{2i-1} \text{ as in (38) replacing } \bar{f} \text{ by } \bar{g}. \end{cases} \qquad (40)$$

5 Numerical experiments.

The purpose of this section is to show how the reconstructions presented in this paper can be used to remove noise.

We consider the function

$$g(x) = \begin{cases} -\frac{4x-3}{5} sin(\frac{3}{2}\pi(\frac{4x-3}{5})^2) & \text{if } 0 \le x < \frac{3\pi}{29}, \\ |sin 2\pi(\frac{4x-3}{5}) + \frac{\pi}{1000}| & \text{if } \frac{3\pi}{29} \le x \le 1. \end{cases} \qquad (41)$$

We discretize $g(x)$ using (4) with $N_L = 2^{5+L}$ obtaining $\bar{g}^L = \{\bar{g}_i^L\}_{i=1}^{N_L}$. Then we obtain $\bar{f}^L = \bar{g}^L + n$, where n is some white Gaussian noise[1].

We consider the *Signal-to-Noise Ratio*, expressed in dB, to measure the noise of the signal:

$$\text{SNR}(g,f) := 10\log_{10}\frac{\sum_{i=1}^{N_L}(\bar{g}_i^L)^2}{\sum_{i=1}^{N_L}(\bar{g}_i^L - \bar{f}_i^L)^2}.$$

[1] Calculated with the function *awgn* of MATLAB ®.

© 2016 NSP
Natural Sciences Publishing Cor.

We fix SNR=25dB and apply L levels of the the direct transform (8), with different reconstructions, to $\{\bar{f}_i^L\}_{i=1}^{N_L}$, obtaining $\{\bar{f}_i^0\}_{i=1}^{N_L/2^L}$. Subsequently, we eliminate all the details $\{d^l\}_{l=1}^{L}$ and we apply L levels of an inverse transform ((9), (31) or (32)) obtaining $\{\hat{f}^L\}_{i=1}^{N_L}$. Then, we evaluate the *Root Mean Squared Error*,

$$\mathrm{RMSE}(\hat{f}^L,\bar{g}^L)=\sqrt{\frac{1}{N_L}\sum_{i=1}^{N_L}(\hat{f}_i^L-\bar{g}_i^L)^2}.$$

In Figure 1-(a) we can see the results that we obtain with the $S\overline{\mathscr{ILSC}}$ reconstruction (Section 3.3.2), using $L=5$, $m=7$ and $r=3$. The noise and the Gibbs phenomenon have been completely removed.

Now we consider the $S\overline{\mathscr{LSC}}$ reconstruction (Section 4.1), with $L=5$, $m=7$ and $r=3$, where the position of the singularity is detected with the function $G_i^{\overline{\mathscr{ILSC}}}(x)$, (21). The imposition of consistency (inverse transform (32)) causes that noise removal is reduced (Figure 1-(b)).

In Figure 1-(c) we use the $S\overline{\mathscr{LSC}-NC}$ reconstruction (Section 4.1) with $L=5, m=7$ and $r=3$. As expected, the location of the jump is lost, but the noise reduction improves with respect $S\overline{\mathscr{LSC}}$.

In Figure 1-(d), we use the $S\overline{\mathscr{ILSC}-\mathscr{LSC}}$ reconstruction (Section 4.2) with $L=5$, $m=7$ and $r=3$. Now, the position of the jump is properly detected and the noise reduction maintained.

Finally, these experimental results are also compared with other image filtering algorithms (VISU [5] and SURE [10]) from *Wavelet Shrinkage Denoising* (see p. ej. [6], [4]), obtaining Figures 1 (e) and (f).

From this experiment we conclude that $S\overline{\mathscr{ILSC}}$ is the best choice considering the RMSE, but $S\overline{\mathscr{ILSC}-\mathscr{LSC}}$ is also a good choice since it provides a closely RMSE and "visually smoother" solutions.

In the second experiment we want to see which parameters (size of the stencil, m, and degree of the polynomial, r) are more adequate to remove noise.

We use $S\overline{\mathscr{ILSC}}$ and $S\overline{\mathscr{ILSC}-\mathscr{LSC}}$ for different noise levels (from 20 to 30 dB) and we evaluate the RMSE between the original data $\bar{g}^5$ and the reconstruction $\hat{f}^5$. The results that we obtain with degree $r=3$ and different size of stencils $m=5,7,9,11,13$ are shown in Figure 2-(a) and (c) for $S\overline{\mathscr{ILSC}}$ and $S\overline{\mathscr{ILSC}-\mathscr{LSC}}$ respectively. When we fix $m=9$ and take different degrees, $r=2,3,4,5$, we obtain the Figure 2-(b) and (d) for $S\overline{\mathscr{ILSC}}$ and $S\overline{\mathscr{ILSC}-\mathscr{LSC}}$ respectively.

We deduce from Figure 2 that we have better results with low degree polynomials for both reconstructions. Regarding the size of the stencil, for $S\overline{\mathscr{ILSC}}$ it is not an important feature, but for $S\overline{\mathscr{ILSC}-\mathscr{LSC}}$ better results are obtained with $m\geq 7$. After testing with some signals, we propose that $r=3$, $7\leq m\leq 15$ is a general good choice.

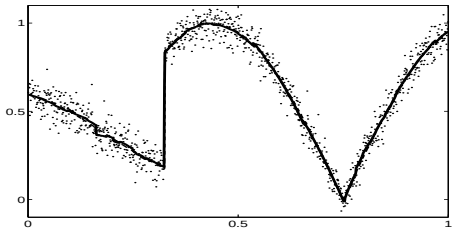

(a) $S\overline{\mathscr{ILSC}}$; RMSE=.017152

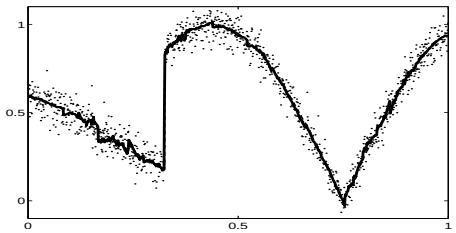

(b) $S\overline{\mathscr{LSC}}$; RMSE=.019001

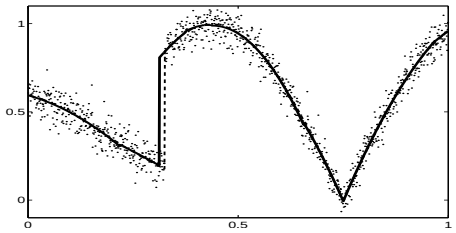

(c) $S\overline{\mathscr{LSC}-NC}$; RMSE=.072368

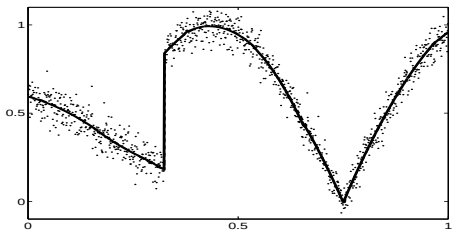

(d)$S\overline{\mathscr{ILSC}-\mathscr{LSC}}$; RMSE=.021364

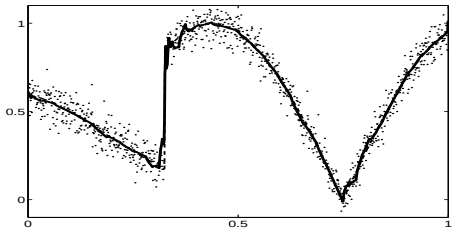

(e) VISU; RMSE=.021185

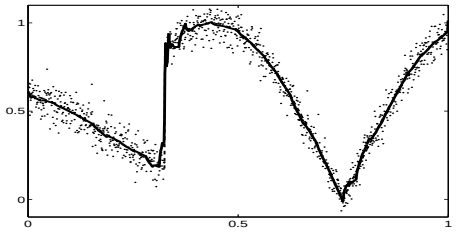

(f) SURE; RMSE=.020157

Fig. 1: We apply 5 levels of decimation and 5 levels of reconstruction without details. We use $r=3$ and $m=7$ from (a) to (d). Dash-dot line represent the original data $\{\bar{g}^5\}$, the dots are the data with noise $\{\bar{f}^5\}$ and the solid line the reconstruction.

© 2016 NSP
Natural Sciences Publishing Cor.

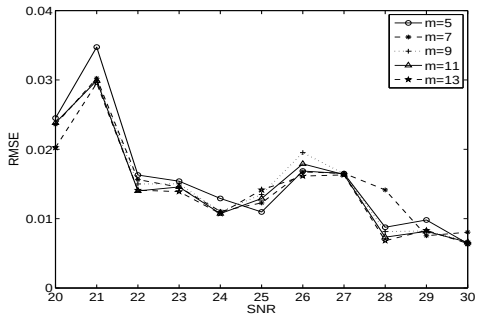

(a) $S\overline{\mathscr{ILSC}}$

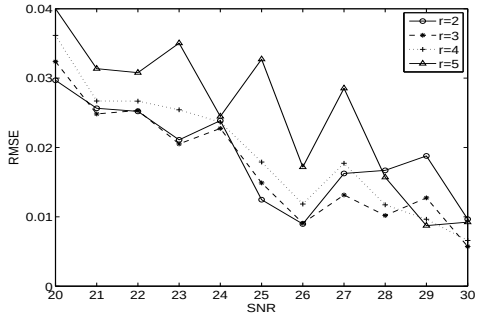

(b) $S\overline{\mathscr{ILSC}}$

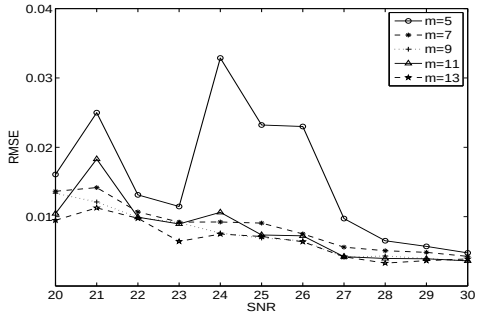

(c) $S\overline{\mathscr{ILSC}-\mathscr{LSC}}$

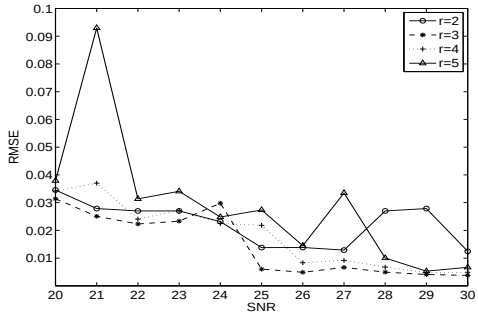

(d) $S\overline{\mathscr{ILSC}-\mathscr{LSC}}$

Fig. 2: For a fixed reconstruction (indicated in each picture), and different magnitude of noise we apply 5 levels of decimation and 5 levels of reconstruction without details. RMSE that we obtain is shown, with degree $r = 3$ and different size of stencils $m = 5,7,9,11,13$ for (a) and (c); and $m = 9$ and different degrees, $r = 2,3,4,5$ for (b) and (d).

In this third experiment we compare the results using the reconstructions $S\overline{\mathscr{ILSC}}$, $S\overline{\mathscr{ILSC}-\mathscr{LSC}}$ (both with $m = 11$ and $r = 3$) and SURE. We decimate L levels and we eliminate all the details $\{d^l\}_{l=1}^{L}$. Afterwards, we apply L levels of an inverse transform. In Figure 3-(a) we show the results that we obtain when $L = 5$ and in Figure 3-(b) when $L = 3$.

We observe that we obtain better results with the $S\overline{\mathscr{ILSC}-\mathscr{LSC}}$ reconstruction, specially when $L = 3$.

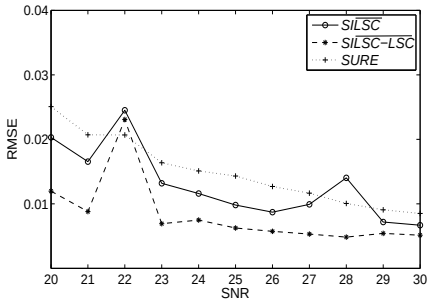

(a)

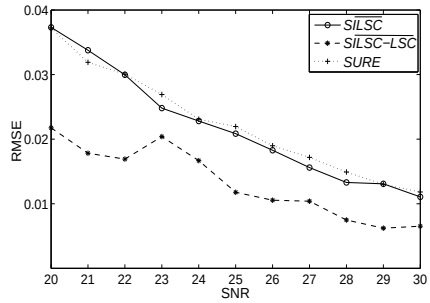

(b)

Fig. 3: Comparison between the methods $S\overline{\mathscr{ILSC}}$, $S\overline{\mathscr{ILSC}-\mathscr{LSC}}$ (eliminating $\{d_i^k\}_{k=1}^{L}$) and SURE. (a) $L = 5$, (b) $L = 3$.

Finally, we show in Figure 4 the limit functions of some reconstructions. We apply 6 levels of reconstruction to $\{\bar{f}_i\}_{i=0}^{15}$ with $\bar{f}_i = 0$, $i \neq 7$, and $\bar{f}_7 = 1$. In (a) we use $\overline{\mathscr{ILSC}}$ and we obtain a broken line. Despite it means that it would be inadequate for using in multiresolution schemes, we have seen in the previous experiments that the results are smooth. This is because we apply the reconstruction to a sufficiently smoothed signal thanks to the cell average decimation. In (b) we use $\overline{\mathscr{LSC}}$ (32), which is consistent. The output is extremely broken, due to the imposition of consistency generates peaks that are transmitted and increased to the next level. With $\overline{\mathscr{LSC}-NC}$ (31), Figure 4-(c), the limit function is smooth since these peaks are not generated.

© 2016 NSP
Natural Sciences Publishing Cor.

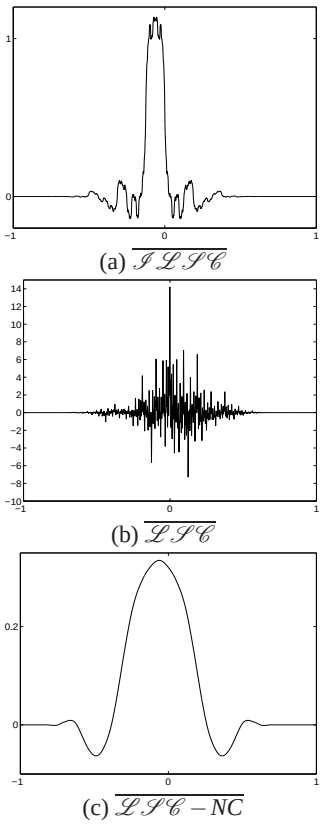

(a) $\overline{\mathscr{I}\mathscr{L}\mathscr{I}\mathscr{C}}$

(b) $\overline{\mathscr{L}\mathscr{I}\mathscr{C}}$

(c) $\overline{\mathscr{L}\mathscr{I}\mathscr{C}-NC}$

Fig. 4: Limit functions. $L = 6$, $m = 7$ and $r = 3$.

6 Conclusions

In this paper we have built a reconstruction, in the cell average framework, based on combining interpolation and least squares approximation (*Interp-*$\mathscr{L}\mathscr{I}$) verifying that it meets the requirements for use in multiresolution schemes *a la Harten*. We have seen how to include the non-linear techniques *ENO* and *SR* in the *Interp-*$\mathscr{L}\mathscr{I}$ reconstruction improving the approximation in the vicinity of discontinuities.

Then, we have presented a reconstruction based on least squares approximations ($\mathscr{L}\mathscr{I}$), also in the cell average framework. In this case we do not have the consistency which is necessary in the multiresolution schemes *a la Harten*. We have presented an scheme that circumvents this problem. While *ENO* can be applied without problems, a way to apply the *SR* in this context is using the function $G_i^{\overline{\mathscr{I}\mathscr{L}\mathscr{I}\mathscr{C}}}(x)$, (21), to detect the singularity (as in section 3.3.2).

We have shown how these reconstructions can be used to reduce the noise. We have compared the results that we obtain with the methods introduced in this paper with other existing techniques. We observe that in the presence of jumps the results we get with the methods presented in this paper ($S\overline{\mathscr{I}\mathscr{L}\mathscr{I}\mathscr{C}}$ and $S\overline{\mathscr{I}\mathscr{L}\mathscr{I}\mathscr{C}-\mathscr{L}\mathscr{I}\mathscr{C}}$) are more accurate in general.

Acknowledgement

This research was partially supported by Spanish MTM 2011-22741 and MTM 2014-54388.

References

[1] F. Aràndiga, A. Cohen, R. Donat, and N. Dyn. Interpolation and approximation of piecewise smooth functions. *SIAM J. Numer. Anal.*, 43(1):41–57, 2005.
[2] F. Aràndiga and R. Donat. Nonlinear multiscale decompositions: the approach of A. Harten. *Numer. Algorithms*, 23(2-3):175–216, 2000.
[3] F. Aràndiga and J. J. Noguera. Signal denoising with Harten's multiresolution using interpolation and least squares fitting. *Advances in Differential Equations and Applications. SEMA SIMAI Springer Series.*, 4:137–145, 2014.
[4] Taswell C. The what, how, and why of wavelet shrinkage denoising. *Comput Sci Eng*, 2:12–9, 2000.
[5] D. L. Donoho. Ideal spatial adaptation by wavelet shrinkage. *Biometrika*, 81(3):425–455, 1994.
[6] D. L. Donoho. Denoising via soft thresholding. *IEEE Transactions on Information Theory*, 41:613–627, 1995.
[7] A. Harten. ENO schemes with subcell resolution. *J. Comput. Phys.*, 83:148–184, 1989.
[8] A. Harten. Multiresolution representation of data: A general framework. *SIAM J. Numer. Anal.*, 33:1205–1256, 1996.
[9] A. Harten, B. Engquist, S. Osher, and S.R. Chakravarthy. Uniformly high-order accurate essentially nonoscillatory schemes. III. *J. Comput. Phys.*, 71(2):231–303, 1987.
[10] I. M. Johnstone and D. L. Donoho. Adapting to smoothness via wavelet shinkage. *Journal of the Statistical Association*, 90(432):1200–1224, 1995.
[11] D. Mizrachi. Remoiving Noise from Discontinous Data. PhD thesis, School of Mathematical Sciences. Applied Math Department, 1991.
[12] J. J. Noguera. Transformaciones multiescala no lineales (http://roderic.uv.es/handle/10550/29285). PhD thesis, Applied Math Department, Univertity of Valencia, 2013 .

Francesc Arandiga was born in Canals, Spain, in 1963. He received the Ph.D. degree in mathematics from the University of Valencia, Valencia, Spain, in 1992. From 1994 to 2010 he has been associate professor and since 2010 full professor of applied mathematics at the University of Valencia. He has been head and secretary of the Department of Applied Mathematics at the University of Valencia. He has also been coordinator of the graduate program in Computer Science and Computational Mathematics. His research interest include image processing, multiresolution analysis, and wavelets. He has published more than 30 research articles in reputed international journals of mathematical and engineering sciences.

© 2016 NSP
Natural Sciences Publishing Cor.

José Jaime Noguera received the PhD degree in Mathematics at Universitat de València (Spain) in 2013. He has published research articles in conferences and journals related to applied mathematics. His research interests include Signal Denoising, Image Compression and Multiresolution Schemes, among others. He currently works in the field of teaching.

© 2016 NSP
Natural Sciences Publishing Cor.